Optics Letters

Ultrafast structured light through nonlinear frequency generation in an optical enhancement cavity

WALKER M. JONES AND MELANIE A. R. REBER*

Department of Chemistry, University of Georgia, Athens, Georgia 30606, USA
**mreber@uga.edu*

Received 29 May 2024; revised 23 July 2024; accepted 6 August 2024; posted 6 August 2024; published 29 August 2024

The generation of shaped laser beams, or structured light, is of interest in a wide range of fields, from microscopy to fundamental physics. There are several ways to make shaped beams, most commonly using spatial light modulators comprised of pixels of liquid crystals. These methods have limitations on the wavelength, pulse duration, and average power that can be used. Here we present a method to generate shaped light that can be used at any wavelength from the UV to IR, on ultrafast pulses, and a large range of optical powers. By exploiting the frequency difference between higher-order modes, a result of the Gouy phase, and cavity mode matching, we can selectively couple into a variety of pure and composite higher-order modes. Optical cavities are used as a spatial filter and then combined with sum-frequency generation in a nonlinear crystal as the output coupler to the cavity to create ultrafast, frequency comb structured light.

https://doi.org/10.1364/OL.531092

Structured light has applications in many areas of science, including microscopy [1], quantum information [2], and fundamental physics [3]. Shaped optical beams have an additional degree of freedom, the spatial mode, and can be used for things such as multimodal entanglement and decreasing quantum noise [4,5]. Recently, there has also been interest in expanding this to spatiotemporal shaped light and in other complex ways [6,7]. There are a wide range of ways to make shaped beams including spatial light modulators [8], q-plates [9], and even in the laser itself [10,11]. Spatial modification of optical beams is most commonly achieved with spatial light modulators where an array of pixels covers the extent of the beam and the shape is modified by turning the pixels on and off. These devices are limited in the resolution of the pixels, which are typically made up of liquid crystals [8] with liquid crystals on silicon as the most common and commercially available [12]. There are also power and wavelength limitations to these methods. The other broad category of methods to create structured light is to generate it directly in the laser cavity. These methods often place an obstruction in the laser cavity to force the cavity to lase in a non-TEM_{00} mode. However, achieving the desired spatial mode while working with the complex nonlinear gain dynamics adds a level of complexity to these methods, and the achievable wavelengths are limited by the gain medium.

Here we present a method to generate shaped light that can be used at any wavelength from the UV to IR, on ultrafast pulses, at a large range of optical powers. Optical cavities are used as the spatial filter and generate shaped laser beams through sum-frequency generation in a nonlinear crystal as the output coupler to the cavity. Higher-order modes have small shifts in their frequencies as a result of the Gouy phase. The cavity resonant frequency can be tuned to select a higher-order mode or group of higher-order modes. Since the cavities are not part of the laser cavity, there is no concern about any effects of or dynamics from the gain medium.

The use of a cavity as a spatial filter and the impact of the cavity on an image were first explored theoretically and experimentally by Gigan *et al.* [13]. They input an image to the cavity, such as a series of slits, and looked at the resultant image after passing through their hemiconfocal cavity. They showed the cavity-transmitted beam was a self-Fourier transform of the image. In this Letter, we use the cavity modes as a spatial filter to shape the incoming light. It has been known for many years that optical cavities support higher-order Hermite–Gaussian beams [14] and that those modes come on resonance with the cavity at different frequencies because of the Gouy phase. Higher-order modes were generally avoided and it is only relatively recently that these have started to be used and researched [15,16]. Using higher-order cavity modes, brought on by the placement of a wire obstruction in the cavity, Weitenberg *et al.* characterized the field with the obstruction in place with the goal to explore the use of a mirror with a hole in it for the output of high harmonic generated light [15,17]. Higher-order modes of optical cavities have also been used to generate squeezed states [5].

In this work, we will exploit the higher-order modes to shape the incoming beam. It is necessary to use a frequency comb laser to couple ultrafast light into an optical cavity [18]. To get the shaped light out of the cavity, we use nonlinear frequency generation in a beta-barium borate (BBO) crystal. Nonlinear frequency generation between frequency comb lasers produces an optical frequency comb, which is well documented [19]. While nonlinear frequency generation has been used in a range

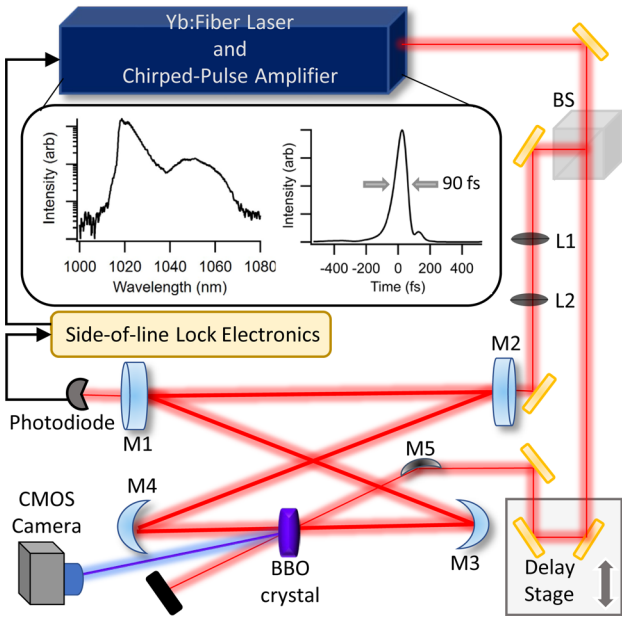

Fig. 1. Experimental setup and laser characterization. A homebuilt ytterbium:fiber laser and chirped-pulse amplifier supply 90 fs pulses at 75 MHz repetition rate centered at 1040 nm. The inset shows an optical spectra and pulse reconstruction. The beam is split into two; one is locked to a bowtie enhancement cavity, and the other is sent to a delay stage. A beta-barium borate (BBO) crystal is placed at the main focus of the cavity where the non-cavity beam, fused by a curved mirror M5, intersects. The resultant SHG beam is sent to a CMOS camera and photodiode for detection.

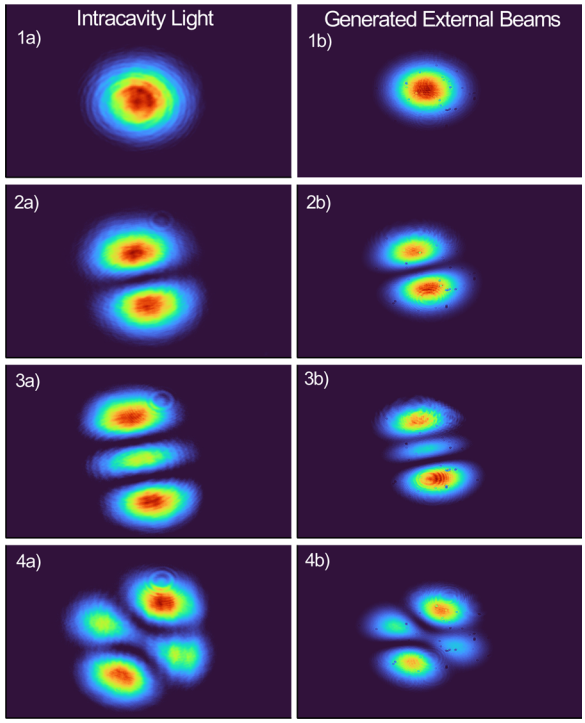

Fig. 2. Pictures of the intracavity modes (a) and the corresponding mode of the generated SHG beam (b). All of these were taken with vertical misalignment into the cavity and a probe beam diameter of 125 μm, which is larger than the cavity beam when they cross. Nominal mode assignments based upon the beam shape are as follows: Panel 1 is a TEM_{00} beam, 2 is a TEM_{10} beam, 3 is a TEM_{20} beam, and 4 is a TEM_{11} beam.

of applications for many years, there are only a few detailed investigations of nonlinear frequency generation with higher-order modes [20–22]. Using nonlinear frequency generation to output the modes from the cavity has not been explored before, to the best of our knowledge.

Specifically, a homebuilt ytterbium:fiber (Yb:fiber) laser frequency comb and amplification system generates 250 mW centered at 1040 nm, a 75 MHz repetition rate, and 90 fs pulses (see Fig. 1). The Yb:fiber laser and amplifier are described in details elsewhere [23,24] and will only briefly be described here. The Yb:fiber oscillator produces about 40 mW pulses of a few picoseconds in duration at a 75 MHz repetition rate. The output of the laser is coupled into the SM980 fiber, which is then spliced to 15 cm of a core pumped, single clad Yb:doped fiber (Thorlabs YB1200-4/125). The doped fiber is forward-pumped by a 500 mW 970 nm diode laser, and the amplified output is then compressed in a double-pass, transmission grating compressor to 90 fs with a 250 mW average power. The amplified output is then split into two paths. One path goes through a set of two lenses to be mode-matched to the optical cavity. The cavity is in a bowtie configuration consisting of two flat mirrors and two curved mirrors with 60 cm focal lengths. The length of the external cavity matches the repetition rate of the laser. The second beam path travels through a computer-controlled delay stage and 25 cm focal length curved mirror. The intra- and extra-cavity foci are spatially overlapped by aligning both through a 25 μm pinhole.

The cavity is locked to the frequency comb using a side-of-line lock. The light transmitted from one of the flat cavity mirrors is incident on a photodetector. The photodetector signal goes to a loop filter board, where it is compared to an adjustable DC voltage. The DC voltage is chosen such that it intersects the transmission peak about two-thirds the way up the peak. This type of lock was chosen over a Pound–Drever–Hall lock or top-of-line lock because of the ease of locking to different modes with large differences in the transmitted light; however, a Pound–Drever–Hall lock can also be used. To lock to a different *TEM* cavity mode involves tuning the length of the cavity to correspond to the desired *TEM* mode frequency and then activating the lock. The lock feeds back onto a piezo attached to one of the cavity mirrors as well as an electro-optic modulator in the laser cavity, as described in detail elsewhere [18].

At the focus of the cavity between the two curved mirrors is a 0.5 mm beta-barium borate (BBO) crystal, chosen because of the nonlinear properties and low dispersion for ultrafast nonlinear processes [25]. The extra-cavity beam crosses the cavity beam at the BBO crystal in an autocorrelation geometry. The two beams undergo second-harmonic generation in the crystal, and a spatially separated second-harmonic beam is emitted in the $\vec{k}_{intra} + \vec{k}_{extra}$ direction. The generated second-harmonic beam is spatially separated from the two infrared beams and sent to a CMOS camera and an amplified photodiode for detection.

By slightly misaligning the input beam of the cavity and varying the distance between the mode-matching lens, a wide range of different spatial modes become resonant in the cavity at different cavity lengths. In practice, the misalignment can be changing the angle of the input beam relative to the cavity, usually not keeping the input beam parallel to the cavity beam, or changing

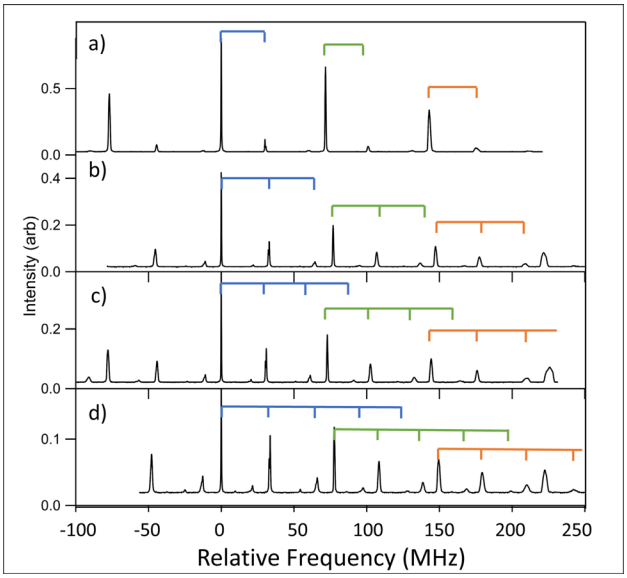

Fig. 3. Transmission spectra of the cavity obtained by scanning the cavity-mirror piezo. The ramp travels through multiple laser repetition rates, with the strongest labeled with the blue track, followed by a green track and then an orange track. Panel (a) shows the spectra of the cavity with very good alignment, so only one higher-order mode appears for each repetition rate. Panels (b)–(d) show the cavity spectra as the input beam is increasingly vertically misaligned causing more higher-order modes to appear.

the beam size on the input mirror. Figure 2 shows a representative set of cavity modes and the corresponding generated beam mode. More cavity output beam shapes are in Fig. S1 in Supplement 1. Vertical misalignment yields more rectangular modes, while coupling a larger beam leads to more higher-order modes with circular symmetry. The spectra of the cavity is obtained by scanning the cavity length using a mirror mounted on a piezo-driven translation stage. Figure 3 shows the optical spectrum of the enhancement cavity, while the cavity input is increasingly misaligned vertically. Panel (a) shows mostly a well-aligned and mode-matched cavity. There are multiple TEM_{00} cavity modes that couple into the cavity, with one labeled by the blue track, one labeled with green, and one with orange. Since the x axis is derived from the piezo voltage, it is calibrated by taking the difference between the peaks and setting that to the repetition rate of the laser as measured on the RF spectrum analyzer. The input frequency comb optical spectrum is broader than what the cavity can support, due to dispersion in air, so we do not see coupling into a single cavity mode but also several nearby cavity modes as seen in Fig. 3. The piezo does not scan perfectly linearly, as can be seen by the slight variation in peak spacing between scans and the broadening of the peaks toward both ends of each scan. The scans were aligned by setting the highest peak to 0 MHz and the average ramp voltage to frequency value as the step to generate the x axis.

Increasing the input beam misalignment relative to the cavity makes it possible to assign the peaks in the cavity spectrum of the most misaligned spectrum [Fig. 3(d)]. When the alignment is done in this way, the strongest modes are clearly the Hermite–Gaussian modes for which the frequencies can be calculated. Specifically, a cavity resonance occurs when the round trip phase shift is 2π or an integer multiple of 2π. Following the derivation of Nagourney Sect. 2.6 [26], the cavity resonant frequencies of the higher-order Hermite–Gaussian modes can be written as follows:

$$\nu_{nmq} = \left(q + (n + m + 1)\frac{cos^{-1}[\pm\sqrt{g_1 g_2}]}{\pi}\right)\frac{c}{L}, \quad (1)$$

where g_1 and g_2 depend upon the cavity parameters, defined as $g_n = 1 - \frac{d_n}{R}$, q is the mode number, and n and m are the Hermite polynomial indices. In the bowtie geometry, R is the radius of curvature of the curved mirrors, d_2 is the length between the curved mirrors, and d_1 is the remaining length of the cavity. The g_n cavity parameters are derived under the assumption that the angles are small and the effects can be neglected. The Guoy phase shift is the $\frac{cos^{-1}[\pm\sqrt{g_1 g_2}]}{\pi}$ term, which depends upon the cavity geometry.

Using this, the difference in the resonant frequency between the adjacent Hermite–Gaussian modes, $\Delta n = 1$, is as follows:

$$\nu_{(n+1)mq} - \nu_{nmq} = \frac{cos^{-1}[\sqrt{g_1 g_2}]}{\pi}\frac{c}{L}, \quad (2)$$

where L is the length of the cavity, c is the speed of light, and g_1 and g_2 are the cavity parameters. It is worth noting that because the resonant frequencies of the Hermite–Gaussian modes go as $n + m + 1$, each mode with the same $n + m$ value will be degenerated (see Fig. S2 in Supplement 1). We are often able to couple predominantly into one mode based upon the incoming beam size and spatial overlap. The difference in resonant frequencies of the different modes is a result of the Gouy phase shift [27].

The cavity used here is a bowtie cavity with 61.1 cm between the curved mirrors (d_1) and 335.5 cm as the remaining cavity length (d_2). The curved mirrors have a 60 cm focal length and all angles are around 5° or less. Using these cavity parameters, we calculate that adjacent higher-order modes are spaced apart by 30.9 MHz. Taking five sets of cavity ramps, fitting the peaks to a Lorentzian function to find the center frequency, and averaging the center frequency, the experimentally measured spacing between modes is 30.8 (1.1) MHz with the standard deviation in parenthesis. For reference the average repetition rate measured this way is 74.3 (3.2) MHz in comparison to 75.367 MHz with the RF spectrum analyzer. This shows that the cavity is behaving as expected and the modes are assignable with the combination of the frequency and beam profile.

The second-harmonic beam shape is a function of the overlap of the two infrared incident beams. The mode structure follows the cavity mode for the larger probe beams. As the probe beam gets smaller, the generated beam changes shape slightly to reflect the overlap with a smaller Gaussian beam. When the probe beam is large, the generated beam reproduces the cavity beam exactly, since the readout beam overfills the Gaussian beam structure, and those are the modes shown in Fig. 2. The efficiency of the generated light increases as the overlap increases and decreases with poorer overlap, as expected. Figure 4 plots the conversion efficiency as a function of the probe beam size. When the probe beam is smaller than the pump beam, there is a strong dependency on the beam size depending upon the cavity mode shape (further details are in Fig. S3 in Supplement 1).

This work demonstrates the use of an optical cavity as a spatial mode filter and how it can be used to create ultrafast structured light. The output beam will be a frequency comb just like the two input beams [19] and have an ultrafast pulse duration [18]. The cavity in this work is in air, which limits the achievable pulse duration in the cavity, but could be

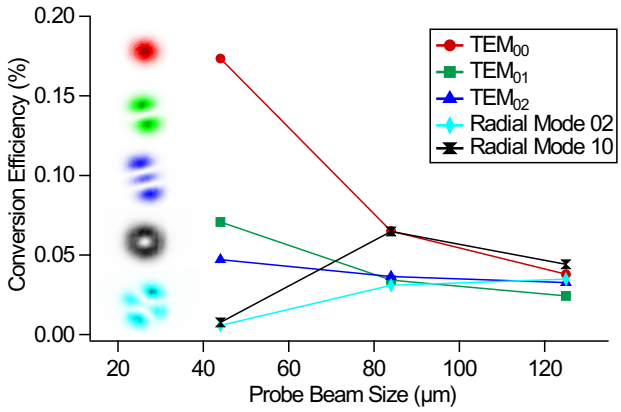

Fig. 4. Conversion efficiency of the different modes while locked at 2/3 peak power as a function of the probe beam (TEM_{00}) size. The three probe beam sizes were chosen to be in the limit of smaller than the cavity beam, about the same size as the cavity beam, and much larger than the cavity beam. The camera images of the cavity beam shape are included on the left, color-coded to match the corresponding data points.

implemented in vacuum or lower dispersion environment. This method is a versatile way to generate ultrafast shaped light and could be applied across an optical spectrum by simply changing the cavity optics and nonlinear crystal. It is also possible to couple light into complex mixed and higher-order modes into the cavity and make complicated shapes, which could be used to generate ultrafast beams with arbitrary shapes. For example, one type of an optical beam that could be generated this way is an ultrafast optical vortex beam, beams with optical angular momentum. One could also image combining two cavities, each locked to different higher-order mode, that cross at the BBO crystal to achieve even more complicated beam shapes and structures [28]. This cavity-based method shows promise as a general method for ultrafast, structured light and structured frequency combs.

Funding. This material is based upon work supported by the National Science Foundation under Grant (2207784); Directorate for Mathematical and Physical Sciences (2207784); University of Georgia Start-up Funds.

Disclosures. The authors declare no conflicts of interest.

Data availability. Data underlying the results presented in this paper are not publicly available at this time but may be obtained from the authors upon reasonable request.

Supplemental document. See Supplement 1 for supporting content.

REFERENCES

1. J. Zeng, Y. Dong, J. Zhang, *et al.*, J. Opt. **25**, 023001 (2023).
2. K. H. Kagalwala, G. Di Giuseppe, A. F. Abouraddy, *et al.*, Nat. Commun. **8**, 739 (2017).
3. A. Forbes, A. Dudley, and M. McLaren, Adv. Opt. Photonics **8**, 200 (2016).
4. K. Wagner, J. Janousek, V. Delaubert, *et al.*, Science **321**, 541 (2008).
5. M. Lassen, V. Delaubert, J. Janousek, *et al.*, Phys. Rev. Lett. **98**, 083602 (2007).
6. Y. Shen, Q. Zhan, L. G. Wright, *et al.*, J. Opt. **25**, 093001 (2023).
7. C. He, Y. Shen, and A. Forbes, Light: Sci. Appl. **11**, 205 (2022).
8. S.-Q. Li, X. Xu, R. M. Veetil, *et al.*, Science **364**, 1087 (2019).
9. A. Rubano, F. Cardano, B. Piccirillo, *et al.*, J. Opt. Soc. Am. B **36**, D70 (2019).
10. A. Forbes, M. de Oliveira, and M. R. Dennis, Nat. Photonics **15**, 253 (2021).
11. A. Forbes, Laser Photonics Rev. **13**, 1900140 (2019).
12. G. Lazarev, P.-J. Chen, J. Strauss, *et al.*, Opt. Express **27**, 16206 (2019).
13. S. Gigan, L. Lopez, N. Treps, *et al.*, Phys. Rev. A **72**, 023804 (2005).
14. H. Kogelnik and T. Li, Appl. Opt. **5**, 1550 (1966).
15. J. Weitenberg, P. Rußbüldt, T. Eidam, *et al.*, Opt. Express **19**, 9551 (2011).
16. L. Djevahirdjian, G. Méjean, and D. Romanini, Meas. Sci. Technol. **31**, 035013 (2020).
17. J. Weitenberg, P. Rußbüldt, I. Pupeza, *et al.*, J. Opt. **17**, 025609 (2015).
18. M. A. R. Reber, Y. Chen, and T. K. Allison, Optica **3**, 311 (2016).
19. A. Schliesser, N. Picque, and T. W. Haensch, Nat. Photonics **6**, 440 (2012).
20. P. Buchhave and P. Tidemand-Lichtenberg, Opt. Express **16**, 17952 (2008).
21. V. Delaubert, M. Lassen, D. Pulford, *et al.*, Opt. Express **15**, 5815 (2007).
22. T. Qi, D. Wang, and W. Gao, Appl. Phys. B **128**, 67 (2022).
23. N. D. Cooper, U. M. Ta, and M. A. R. Reber, Appl. Opt. **62**, 2195 (2023).
24. W. M. Jones, P. Nyaupane, and M. A. R. Reber, in preparation.
25. J. Y. Zhang, J. Y. Huang, H. Wang, *et al.*, J. Opt. Soc. Am. B **15**, 200 (1998).
26. W. Nagourney, *Quantum Electronics for Atomic Physics and Telecommunication*, 2nd ed (Oxford University Press, 2014).
27. A. E. Siegman, *Lasers* (University Science Books, 1982).
28. D. Shen, T. He, X. Yu, *et al.*, IEEE Photonics J. **14**, 1 (2022).